

# Lawrence Berkeley National Laboratory

## Recent Work

### Title

COUPLED CHANNEL ALPHA DECAY RATE THEORY APPLIED TO  $^{212}\text{Po}$

### Permalink

<https://escholarship.org/uc/item/3s06s8dv>

### Authors

Rauscher, E.  
Rasraussen, J.O.  
Harada, K.

### Publication Date

1966-10-01

UCRL-16351

University of California  
Ernest O. Lawrence  
Radiation Laboratory

COUPLED CHANNEL ALPHA DECAY RATE THEORY  
APPLIED TO  $^{212m}\text{Po}$

TWO-WEEK LOAN COPY

*This is a Library Circulating Copy  
which may be borrowed for two weeks.  
For a personal retention copy, call  
Tech. Info. Division, Ext. 5545*

Berkeley, California

## **DISCLAIMER**

This document was prepared as an account of work sponsored by the United States Government. While this document is believed to contain correct information, neither the United States Government nor any agency thereof, nor the Regents of the University of California, nor any of their employees, makes any warranty, express or implied, or assumes any legal responsibility for the accuracy, completeness, or usefulness of any information, apparatus, product, or process disclosed, or represents that its use would not infringe privately owned rights. Reference herein to any specific commercial product, process, or service by its trade name, trademark, manufacturer, or otherwise, does not necessarily constitute or imply its endorsement, recommendation, or favoring by the United States Government or any agency thereof, or the Regents of the University of California. The views and opinions of authors expressed herein do not necessarily state or reflect those of the United States Government or any agency thereof or the Regents of the University of California.

Submitted to Nuclear Physics

UCRL-16351

UNIVERSITY OF CALIFORNIA

Lawrence Radiation Laboratory  
Berkeley, California

AEC Contract No. W-7405-eng-48

COUPLED CHANNEL ALPHA DECAY RATE THEORY APPLIED TO  $^{212}\text{Po}$

E. Rauscher, J. O. Rasmussen, and K. Harada

October 1966

COUPLED CHANNEL ALPHA DECAY RATE THEORY APPLIED TO  $^{212m}\text{Po}^*$

E. A. Rauscher<sup>†</sup> and J. O. Rasmussen

Lawrence Radiation Laboratory and  
Chemistry Department  
University of California  
Berkeley, California

and

K. Harada

Japan Atomic Energy Research Institute  
Tokai-Mura, Japan

Abstract

A new application of the coupled channel formalism is made for the case of the alpha decay of the high spin,  $J=18+$  state of  $^{212}\text{Po}$  to the ground state and various excited states of  $^{208}\text{Pb}$ . In the first part of this paper (Sec. 2), we apply the microscopic or "shell model" rate theory neglecting coupling. It is found that the theory underestimates both the experimental 1% alpha branch to the 3-, first excited state of  $^{208}\text{Pb}$  and the 2% branch to the second, 5- state, for connection radius,  $R=9$  Fm. Choice of a small  $R$  of 7.5 Fm results in a satisfactory agreement for the branching to the 5- state but leaves a discrepancy of over an order of magnitude for the branch to the 3- state.

In the second part of this paper (Secs. 3,4,5), we solve the radial Schrödinger equations for  $L=18$  and  $L=15$  waves coupled by the collective octupole vibrational field. We show that the channel coupling has a substantial effect on over-all barrier penetrability, but that coupling does not help much

in removing the underestimate of the  $3^-$  intensity for  $R \geq 7.5$  Fm for the parameters we used. It is suggested that neglected octupole core polarization in parent nuclear wave functions may be responsible for the remaining discrepancy.

---

† Present address: Lawrence Radiation Laboratory, Livermore, California

### 1. Introduction

In the first part of the paper we apply shell model rate theory <sup>1)</sup> and simple barrier penetrability calculations to  $^{212m}\text{Po}$ . In the second part we consider the effects of collective octupole coupling between different channels in the alpha decay.

Macroscopic theory in its ordinary form of a particle in a potential well yields alpha decay rates roughly proportional to a Coulomb barrier penetration factor arising from the solution of a separate Schrödinger equation for each alpha group of given  $L$  value. Preston early considered <sup>2)</sup> the effects of considering the coupling arising from the electromagnetic field associated with transitions between various states of the daughter nucleus, these considerations led to sets of coupled second order linear differential equations.

The coupling effects have been studied extensively for the rotational states of deformed nuclei, where such effects are predominantly due to the large collective E2 transition strengths and the small energy differences between various rotational states <sup>3)</sup>.

The magnitude of the coupling terms for alpha particle outside the range of nuclear forces is uniquely related to the reduced electric transition probability between the states in question (cf. eq. (6.3) of ref. 3).

It is well known that one-body alpha decay theory, even when augmented by the treatment of interchannel coupling, is inadequate to explain even the relative intensities of alpha decay to various excited states of daughter nuclei <sup>4)</sup>. The "microscopic" or shell model theoretical approach of Mang has

proved remarkably successful in calculating alpha relative intensities in spherical nuclei (Bi, Po region) without regard to interchannel coupling <sup>5)</sup> and in spheroidal nuclei <sup>6)</sup>, taking such coupling into account by Fröman's matrix method <sup>7)</sup>. It is necessary to specify a nuclear surface, characterized by a radius  $R_0$ , where the alpha wave function of the inner region joins that of the outer. Fortunately, relative rates of the theory appear usually not sensitive to the exact choice of  $R_0$ .

## 2. Alpha Rate Theory Neglecting Channel Coupling

We study here a case in the region of spherical nuclei where the shell-model theoretical method without interchannel coupling has difficulty with the relative alpha intensities and where the results appear sensitive to the choice of  $R_0$ . This case is the remarkable super-high-spin isomer of  $^{212}\text{Po}$ , which we now believe to be spin 18, even parity, on the basis of recent shell model calculations <sup>8)</sup>.

The experimental alpha decay energies and intensities <sup>9)</sup> for  $^{212m}\text{Po}$  are summarized in Fig. 1.

This alpha emitter is unusual in that the angular momentum values in the alpha decay are so high. Suppose we take the following alpha-nuclear potential, which is the real part of a potential used for optical model fits of alpha elastic scattering angular distributions:

$$V_N(r) = \frac{-V_0}{1 + \exp \frac{r - r_0 A^{1/3} - a}{d}} \quad (1)$$



with  $V_0 = 35.0$  MeV,  $R_0 = 1.17$  Fm,  $a = 2.17$  Fm, and  $d = 0.576$  Fm. The resulting effective potentials in the radial wave equation for various alpha partial waves are plotted in Fig. 2. The alpha decay energy of  $^{212m}\text{Po}$  is 11.65 MeV, and we see that we are confronted with the unusual situation of the absence of an inner classical turning point for the  $L = 18$  partial wave, because the inner minimum potential energy is more than 27 MeV. The same is true of the lower energy groups to the 3- and 5- excited states.

The alpha-decay barrier width and hence barrier penetrability, as calculated using realistic optical potentials, is curiously undefined. To be sure, if we used a Woods-Saxon nuclear potential with well depth  $V_0$  exceeding 50 MeV, the inner turning points would reappear, but the arbitrariness of the problem remains. Optical model analyses for alpha scattering have been unable to determine very well the potential in the nuclear interior, because alpha particles have such short mean free-path in nuclear matter that alpha scattering does not sample the nuclear interior but only the surface region.

During the final stage of writing this paper the thorough alpha optical model analysis of Mc Fadden and Satchler was published<sup>10)</sup>. Their work favors very deep potentials of the order of 200 MeV, and would have used their potentials if we had known of them earlier.

Let us first apply simple microscopic alpha decay rate theory without channel coupling to this case.

For the 3- first excited state of  $^{208}\text{Pb}$  calculations based on the random phase approximation (RPA) have been made by Gillet et al.<sup>11)</sup>. The RPA method admixes 2 particle-2 hole (2P - 2H) states into the ground state wave

function of  $^{208}\text{Pb}$ , and  $3\text{P} - 3\text{H}$  states into the  $3^-$  state function in addition to the  $1\text{P} - 1\text{H}$  states. Since the ground state core correlations were not included in the  $^{212\text{m}}\text{Po}$  wave functions<sup>8)</sup> we shall use, the use of the  $^{208}\text{Pb}$  wave functions obtained by usual Tamm-Dancoff shell theory are more consistent in what follows. Two different shell model wave functions for the  $3^-$  state of  $^{208}\text{Pb}$  were available to us. One is calculated by Pinkston<sup>12)</sup>, and another is by True and Pinkston<sup>13)</sup>. The former could not reproduce the correct energy, but in the latter True succeeded in getting a nice agreement by taking into account twenty  $1\text{P} - 1\text{H}$  configurations. He included  $4s_{1/2}$ ,  $2g_{7/2}$ , and  $3d_{3/2}$  neutron levels in his particle configurations, while they were neglected in the shell model calculations<sup>8)</sup> on  $^{212}\text{Po}$ . Among the many configurations in  $^{212\text{m}}\text{Po}$  involving the above neutron orbitals only the following four configurations can have spin 18:  $[(i_{13/2})^2(g_{7/2})^2]$ ,  $[(i_{13/2})^2(g_{9/2}g_{7/2})]$ ,  $[(i_{13/2})^2(i_{11/2}g_{7/2})]$  and  $[(i_{13/2})^2(d_{5/2}g_{7/2})]$ . (The proton configuration is written first, then the neutron.) Since the amounts of the mixing of those components in the isomeric state would surely be very small, we may use True's  $3^-$  state wave function as is for our calculations. To facilitate comparison with earlier alpha rate calculations of Zeh<sup>14)</sup> we list the principal components ( $>1\%$ ) in parent and daughter wave functions.

$$\begin{aligned}
 \chi_{18+} (^{212\text{m}}\text{Po}) = & -0.810 | (h_{9/2})_3^2 (g_{9/2}i_{11/2})_{10} \rangle \\
 & -0.570 | (h_{9/2}f_{7/2})_8 (g_{9/2}i_{11/2})_{10} \rangle \\
 & +0.104 | (h_{9/2})_3^2 (i_{11/2})_{10}^2 \rangle \\
 & +24 \text{ smaller components}
 \end{aligned}$$

$$\begin{aligned}
 \chi_{3-}^{(208}\text{Pb})(\text{ref. 12}) &= -.124|f_{5/2}^{-1}g_{9/2}\rangle_N + .616|f_{5/2}^{-1}i_{11/2}\rangle_N \\
 &+ .737|d_{3/2}^{-1}h_{9/2}\rangle_P + .237|s_{1/2}^{-1}f_{7/2}\rangle_P \\
 &+ 1 \text{ component } (< .1)
 \end{aligned}$$

$$\begin{aligned}
 \chi_{3-}^{(208}\text{Pb})(\text{ref. 13}) &= -.166|f_{5/2}^{-1}g_{9/2}\rangle_N + .431|p_{3/2}^{-1}g_{9/2}\rangle_N \\
 &+ .528|d_{3/2}^{-1}h_{9/2}\rangle_P + .396|f_{5/2}^{-1}i_{11/2}\rangle_N \\
 &- .120|p_{1/2}^{-1}d_{5/2}\rangle_N + .375|s_{1/2}^{-1}f_{7/2}\rangle_P \\
 &- .151|d_{3/2}^{-1}f_{7/2}\rangle_P + .182|f_{7/2}^{-1}g_{9/2}\rangle_N \\
 &+ .227|i_{13/2}^{-1}j_{15/2}\rangle_N + .183|p_{1/2}^{-1}g_{7/2}\rangle_N \\
 &+ .135|f_{5/2}^{-1}g_{7/2}\rangle_N + 9 \text{ components } (< 0.1)
 \end{aligned}$$

$$\begin{aligned}
 \chi_{5-}^{(208}\text{Pb})(\text{ref. 13}) &= -.801|p_{1/2}^{-1}g_{9/2}\rangle_N - .131|f_{5/2}^{-1}g_{9/2}\rangle_N \\
 &+ .250|p_{1/2}^{-1}i_{11/2}\rangle_N + .320|s_{1/2}^{-1}h_{9/2}\rangle_P \\
 &+ .144|p_{3/2}^{-1}g_{9/2}\rangle_N + .225|d_{3/2}^{-1}h_{9/2}\rangle_P \\
 &+ .171|f_{5/2}^{-1}i_{11/2}\rangle_N - .185|d_{3/2}^{-1}f_{7/2}\rangle_P \\
 &+ .105|p_{3/2}^{-1}g_{3/2}\rangle_N + 11 \text{ components } (< 0.1)
 \end{aligned}$$

Adopting the approximation of the small alpha size limit <sup>15)</sup>, we get the following expression for the reduced width amplitude  $\gamma_\alpha$  at the radius R,

$$\begin{aligned} \gamma_\alpha &= \frac{\hbar^2}{2\mu} \sqrt{2j} \langle (j_1 j_2)^{J_p} (j_3 j_4)^{J_n} JM | \cdot \chi_{\alpha m} \sum_{LJM-m} (LJM-m | JM) Y_{LM-m}(\hat{R}) \times | j_4, j_5^{-1}; jm \rangle dx_N dx_\alpha d\Omega_R \\ &= C \cdot 2 N_{j_1 j_2} N_{j_3 j_4} \sum_{J_n} (-)^{(j_2 - 1/2 - 1/2) + (j_5 - 1/2 - 1/2)} \frac{1}{\sqrt{[j_1][j_2][j_3][j_4][j_5][J_n][J_n][j]}} \\ &\times (j_1 j_2 1/2 - 1/2 | J_p 0) (j_3 j_4 1/2 - 1/2 | J_n 0) (J_p J_n' 0 | L 0) \\ &\times (-)^{j_4 + j_5 + J_n + J_n'} W(j_3 j_4 J_n' j; J_n j_5) W(j J_n' J J_p n L) \\ &\times R_1(R) R_2(R) R_3(R) R_5(R) \end{aligned} \tag{2}$$

where C is a constant independent of nuclear structure,  $R_i(a)$  is the value of the i-th particle wave function at the radius R;  $[j_1]$  stands for  $2j_1+1$ ; and

$N_{ij}$  is

$$\begin{aligned} N_{ij} &= \sqrt{2} \quad \text{for } i \neq j \\ &= 1 \quad \text{for } i = j \end{aligned}$$

We have used for numerical calculation the radial wave functions of Blomqvist and Wahlborn<sup>16</sup>) evaluated at a radius "R" of 9.5 Fm. The results of our numerical calculations are summarized in Table I.

The usual definition of barrier penetrability factor is  $[F_L^2(R_0) + G_L^2(R_0)]^{-1}$ , where F and G are the regular and irregular Coulomb functions, or their continuations in the presence of a nuclear potential. For our cases  $F_L^2 \ll G_L^2$  and  $F_L^2$  is ignored. The first order WKB approximation for this penetrability is as follows:

$$1/G_L^2(R_0) \approx \frac{k_L}{\xi_L} \exp \left[ -2 \int_R^{R_t} \frac{2\mu(V_L - Q)}{\hbar} dr \right] \quad (3)$$

where  $\xi_L = \frac{[2\mu(V_L(R)) - Q]^{1/2}}{\hbar}$ .

We define a "zeroth order" penetrability factor differing in that it drops the pre-exponential factor, which has a troublesome singularity as a feature of the first order WKB approximation at the inner classical turning point. Thus our

Table I. Shell-Model Theoretical Alpha Reduced Transition Matrix Elements and their squares. (Radius  $R=9.5$  fm)

$^{212m}\text{Po}(18+) \rightarrow ^{308}\text{Pb}(0+)$	L	$\gamma_{\alpha L}$	$\gamma_{\alpha L}^2$
	13	+0.556	0.309
$\rightarrow ^{208}\text{Pb}(3-)$ (ref.12)	15	-0.2039	0.0416
$\rightarrow ^{208}\text{Pb}(3-)$ (ref.13)	15	-0.0720	0.0052
	17	+0.0326	0.0011
	19	+0.0005	0.0000
	21	-0.0000	0.0000
$\rightarrow ^{208}\text{Pb}(5-)$ (ref.13)	13	+0.3284	0.1078
	15	+0.0156	0.0002
	17	-0.0020	0.0000
	19	+0.0001	0.0000
	21	-0.0001	0.0000
	23	intrinsically forbidden	

barrier penetrability factor distinguished by the superscript zero, is simply the exponential function of argument twice the WKB integral from outer turning point  $R_t$  to the radius  $R$ .

$$P_L^{(0)}(Q,R) = \exp \left[ -2 \int_R^{R_t} \frac{2\mu(V_L - Q)}{\hbar} \right] \quad (4)$$

where  $V_L$  is the sum of coulomb and nuclear potentials, as follows:

$$V_L(r) = \frac{2Ze^2}{r} + \frac{\hbar^2(I+1/2)^2}{2\mu r^2} - V_N(r)$$

with  $V_N(r)$  as defined by Eq. (1), with the same parameters (35 MeV Nuclear Potential) as used for Fig. 2. In Table II are given the penetrability factors according to Eq. (4) for all possible partial waves to the  $0_+$ ,  $3_-$ , and  $5_-$  states of  $^{208}\text{Pb}$ , evaluated at several values of the lower limit  $R$ . Also given are S-wave penetrabilities for  $^{212}\text{Po}$  ground state decay. To give some feeling for the uncertainties in absolute penetrabilities associated with our uncertainties about the nuclear potential, we give in Table III a few penetrability values calculated with the deeper potential finally chosen by Poggenburg for his theoretical calculations <sup>6</sup>). ( $V_0 = -74.0$  MeV,  $r_0 = 1.17$  Fm,  $a = 1.6$  Fm, and  $d = 0.565$  Fm, are the parameters for eq. (1).) In what follows we shall use only the penetrabilities of Table II.

By definition of the reduced width  $\gamma_L^2$  the partial decay rates are given <sup>17)</sup>

by

Table 2

"Zeroth-order-WKB" barrier penetration factors at various radii  $V_0=35$  MeV.

$Q_\alpha$ (MeV)	L	$R_0$ (m)	7	7.5	8	9.5
			<u>Isomer Decay</u>			
11.906	18	6.640(-24)	9.725(-22)	7.558(-21)	4.394(-20)	9.293(-18)
9.291	15	1.984(-25)	1.245(-23)	6.310(-23)	2.591(-22)	2.497(-20)
9.291	17	2.867(-28)	3.623(-26)	2.604(-25)	1.513(-24)	3.240(-22)
9.291	19	3.148(-31)	7.850(-29)	7.846(-28)	6.284(-27)	2.899(-24)
9.291	21	2.598(-34)	1.262(-31)	1.732(-30)	1.883(-28)	1.837(-26)
8.720	13	3.060(-24)	9.832(-23)	3.533(-22)	1.026(-21)	4.784(-20)
8.720	15	5.474(-27)	3.609(-25)	1.895(-24)	8.080(-24)	8.655(-22)
8.720	17	7.612(-30)	1.006(-27)	7.425(-27)	4.446(-26)	1.041(-23)
8.720	19	7.897(-33)	2.048(-30)	2.094(-29)	1.721(-28)	8.359(-26)
8.720	21	6.091(-36)	3.061(-33)	4.288(-32)	4.770(-31)	4.988(-28)
8.720	23	< (-38)	3.397(-36)	6.467(-35)	9.642(-34)	2.091(-30)
			<u>Ground State Decay</u>			
8.729	0	*	*	*	*	4.295(-14)

\* Penetrability at inner turning point of 9.124 Fm is  $2.706 \cdot 10^{-14}$ .



Table 3  
 "Zeroth-order-WKB" barrier penetration factors at inner t.p. and 9.5 Fm  $V_0 = 74.0$  MeV.

	$Q_\alpha = 11.906$ MeV				$Q_\alpha = 8.720$ MeV	
	$R_0$ (Fm) i.t.p.	$P_L$	$R_0$ (Fm) i.t.p.	$P_L$	$R_0$ (Fm) i.t.p.	
L=18	8.368	3.209(-19)				
	9.5	8.305(-18)				
L=13					8.712	6.196(-21)
					9.5	4.218(-20)
L=15			8.573	1.898(-21)	8.551	5.978(-23)
			9.5	2.217(-20)	9.5	7.697(-22)
L=17			8.374	1.100(-22)	8.349	3.168(-25)
			9.5	2.901(-22)	9.5	9.334(-24)
L=19			8.087	3.265(-26)	8.053	8.455(-28)
			9.5	2.615(-24)	9.5	7.754(-26)
L=21			7.5*	2.932(-28)	7.5	6.799(-31)
			9.5	1.668(-26)	9.5	4.534(-28)
L=23					7.5	5.970(-34)
					9.5	1.912(-30)
L=0					9.220	2.498(-14)
					9.5	3.596(-14)

\* Inner turning point is < 6.0 Fm for the L = 21 and L = 23 waves.

$$\lambda_L = \frac{2\gamma_L^2}{\hbar} \frac{\xi_L}{(F_L^2 + G_L^2)} \approx \frac{2\gamma_L^2 k_L}{\hbar} P_L^{(0)} \quad (5)$$

or are proportional to the product of  $\gamma_L^2$  from Table I,  $P_L^{(0)}$  at 9.5 Fm in the last column of Table II, and the wave number,  $k_L$ . It is readily seen that the theory predicts that partial waves of higher  $L$  than the lowest value are never more than a few tenths of a percent. If we ignore higher partial waves, the theory predicts an alpha intensity ratio as follows at  $R$  of 9.5 Fm:

$$\frac{I(18+ \rightarrow 3-)}{I(18+ \rightarrow 0)} = 4.0 \times 10^{-5} \text{ (ref. 13), or } 3.2 \times 10^{-4} \text{ (ref. 12)}$$

to be compared with the experimental ratio of  $1.0 \times 10^{-2}$ .

In similar fashion we get theoretically the following:

$$\frac{I(18+ \overset{13}{\rightarrow} 5-)}{I(18+ \overset{13}{\rightarrow} 0+)} = 1.5 \times 10^{-3} \text{ (ref. 13)}$$

to be compared with the experimental ratio of  $2.1 \times 10^{-2}$ .

Before we turn to channel coupling in an attempt to understand these serious discrepancies, let us consider the effect of a smaller connection radius "R". Because of the very high  $L$  values involved, there is a considerable sensitivity to "R" for the predicted intensity ratios. Using Blomqvist-Wahlborn radial functions for  $R = 7.5$  Fm instead of 9.5 Fm and otherwise the same parameters as for calculations of Table I, we find only moderate changes in the ratio  $\gamma^2(18+ \overset{13}{\rightarrow} 5-)/\gamma^2(18+ \overset{18}{\rightarrow} 0+)$  specifically a decrease of 29% for the wave function of ref. 13 and an increase of 15% for that of ref. 12 in going from 9.5 Fm to 7.5 Fm. For the ratio  $\gamma^2(18+ \overset{13}{\rightarrow} 5-)/\gamma^2(18+ \overset{13}{\rightarrow} 0+)$  there is an increase of 16%.

By inspection of Table II one sees that the relative values of barrier penetrability change very markedly for a similar change of  $R$ . We get the following revised theoretical intensity ratios at  $R = 7.5$  Fm

$$\frac{I_{18+ \rightarrow 3-}}{I_{18+ \rightarrow 0+}} \approx 1.0 \times 10^{-4} \quad (\text{ref. 13})$$

or

$$1.3 \times 10^{-3} \quad (\text{ref. 12})$$

$$\frac{I_{18+ \rightarrow 5-}}{I_{18+ \rightarrow 0+}} \approx 1.9 \times 10^{-2} \quad (\text{ref. 13})$$

We see that the latter theoretical intensity ratio (decay to 5-) is completely in agreement with experiment for  $R = 7.5$  Fm, but the theoretical relative intensity to the 3- state is still one or two orders of magnitude too small, depending on which daughter wave functions are used.

Note also that in the paper of Glendenning and Harada<sup>8)</sup> that the microscopic alpha rate calculations gave too large an isomeric decay rate relative to ground decay rate, i.e., a discrepancy factor of 45 at  $R = 9.5$  Fm and 18 at  $R = 9.0$ . Rasmussen has given formulas<sup>3)</sup> for microscopic theory with  $R$  inside the inner turning point; using this approach and considering roughly that the effective penetrability factor is constant at  $2.7 \times 10^{-14}$  for ground decay for  $R < 9.124$  Fm (see Table II), perfect agreement with experiment is obtained around  $R = 8$  Fm, and at smaller radii the disagreement is of the opposite sense. Here we have assumed the ratios of  $\gamma^2$  values to be nearly independent of radius.

The indications are that a joining radius  $R$  in the neighborhood of 7.5 - 8.5 Fm is more nearly correct with the shell-model nuclear wave functions employed. However, even with  $R$  values in this vicinity the underestimate of decay intensity to the  $3^-$  state is serious. Our difficulty is probably consistent with the results<sup>14)</sup> of Zeh, who found for several combinations of unmixed shell-model initial and final states that the theoretical fraction of alpha decay to the  $3^-$  was too low. Two of his three combinations giving agreement with theory are only minor contributors in the configuration mixed wave functions we used, but one, namely  $((h_{9/2})^2_{8P}(g_{9/2}^i h_{11/2})_{10N})_{18}$  initial and  $|d_{3/2}^{-1} h_{9/2}\rangle_P$  final would be given large weight in our wave functions. Perhaps the main reason our discrepancy is less with the early fewer-term  $3^-$  wave function of ref. 12 is that the  $|d_{3/2}^{-1} h_{9/2}\rangle_P$  configuration has a larger relative amplitude in that case.

### 3. Alpha Rate Theory with Electromagnetic Coupling

We propose here to explore the possibility that interchannel coupling due to the collective electric octupole transition in  $^{208}\text{Pb}$  affects significantly the theoretical decay rate to the  $3^-$  state. We consider at first only the two channels  $l = 18$  and  $l = 15$ . The wave function is of form

$$\Psi_M = \frac{u_{18}(r)}{r} Y_{18}^M(\omega) X_0^0 + \frac{u_{15}(r)}{r} \sum_m (15 \ 3 \ m \ M-m | 13 \ M) Y_{15}^m X_3^{M-m}$$

where  $X_j^{M_j}$  is the daughter nuclear wave function and  $Y_L^m$  is the spherical harmonic of the alpha angular position. Upon substitution into the Schrödinger equation and integration over all variables except  $r$  we get the following coupled radial equations to be solved:

(consider  $r \geq 12$  Fm, i.e., alpha outside the range of nuclear forces)

$$\frac{d^2 u_{18}}{dr^2} - \left\{ \frac{2\mu}{\hbar^2} \left[ \frac{2Ze^2}{r} - Q_{18} \right] + \frac{18.19}{r^2} \right\} u_{18} = K_{03} u_{15} \quad (6a)$$

$$\frac{d^2 u_{15}}{dr^2} - \left\{ \frac{2\mu}{\hbar^2} \left[ \frac{2Ze^2}{r} - Q_{15} \right] + \frac{15.16}{r^2} \right\} u_{15} = K_{03} u_{18} \quad (6b)$$

where  $u_l$  is  $r$  times the radial function of the  $l^{\text{th}}$  partial wave,  $\mu$  is the reduced mass,  $Q_l$  is the decay energy. The  $E3$  reduced transition probability,  $B(E3)$  is calculated<sup>18)</sup> to be  $4.8 \times 10^4 e^2 \text{Fm}^6$  from the experimentally measured half life of  $3 \times 10^{-11}$  sec for the  $3^-$  state. The electromagnetic

coupling constant,  $K_{03}$ , is given <sup>3)</sup> in general for distances  $r > R_0$  as

$$K_{\ell I_f \ell' I'_f}^\lambda(r) = (-)^{I'_f - I} \frac{2\mu}{\hbar^2} \frac{2e[(2\ell+1)(2\ell'+1)4\pi(2I_f'+1)B_{I_f \rightarrow I_f'}(E\lambda)]^{1/2}}{r^{\lambda+1}(2\lambda+1)} \quad (7)$$

$$\times (\ell \ell' 00 | \lambda 0) W(\ell I_f \ell' I'_f; I \lambda).$$

Following eq. (12) later we discuss the choice of sign associated with the  $[B(E\lambda)]^{1/2}$ . We choose the method <sup>19)</sup> of inward numerical integration with boundary conditions at large distance restricted by the experiment relative intensities. None of the usual analytical approximations to solution of these equations seems suitable, since the diagonal energy differences become large on either side of the crossover distance. Therefore, we have chosen to carry out numerical integrations by the Runge-Kutta method using the IBM-7094 computer of the Lawrence Radiation Laboratory in Berkeley. The complete set of four linearly independent solutions is computed by the four boundary conditions at 40.0 Fm given in Table IV. The quantities,  $G_L$  and  $F_L$ , of course, denote the standard irregular and regular coulomb functions, respectively, with the arguments  $\eta$  and  $\rho$  appropriate to the decay energy in each case. The general solution may be expressed as a linear combination of these basis solutions.

Table 4

Boundary Conditions for the Coupled Equations

	<u>Set I</u>	<u>Set II</u>	<u>Set III</u>	<u>Set IV</u>
$u_{18}$	$G_{18}$	$F_{18}$	0	0
$\frac{du_{18}}{dR}$	$k_{18} \frac{dG_{18}}{d\rho}$	$k_{18} \frac{dF_{18}}{d\rho}$	0	0
$u_{15}$	0	0	$G_{15}$	$F_{15}$
$\frac{du_{15}}{dR}$	0	0	$k_{15} \frac{dG_{15}}{d\rho}$	$k_{15} \frac{dF_{15}}{d\rho}$

The desired solutions for the alpha decay problem behave asymptotically like outgoing coulomb waves, although there may be additional phase shifts  $\delta_{18}$  and  $\delta_{15}$  arising from the coupling. That is,

$$u_{18} \rightarrow A[G_{18}(k_{18}r) + iF_{18}(k_{18}r)]e^{i\delta_{18}} \quad (8a)$$

$$u_{15} \rightarrow B[G_{15}(k_{15}r) + iF_{15}(k_{15}r)]e^{i\delta_{15}} \quad (8b)$$

The solutions are to be joined at the nuclear surface with quasi-stationary state solutions, in which the real components vastly dominate over the imaginary components.

Let us denote the components of the basis set of solutions as  $u_{18}^{(I)}$ ,  $u_{15}^{(I)}$ ,  $u_{18}^{(II)}$ ,  $u_{15}^{(II)}$  etc. Then the above conditions at the nuclear surface are essentially expressed by the equations for both  $L$  values setting the imaginary components to zero,

$$\begin{aligned} \text{Im}(u_L) &= A[\sin \delta_{18} u_L^{(I)}(R_0) + \cos \delta_{18} u_L^{(II)}(R_0)] \\ &+ B[\sin \delta_{15} u_L^{(III)}(R_0) + \cos \delta_{15} u_L^{(IV)}(R_0)] = 0. \end{aligned} \quad (9)$$

The other two equations necessary to solve for the four real quantities  $A, B, \delta_{18}$ , and  $\delta_{15}$  may be either supplied near the nuclear surface by a microscopic nuclear model, or in the approach we use a large-distance boundary condition fixed by experimental alpha decay rates.

Let  $\lambda_{18}$  and  $\lambda_{15}$  be the partial decay constants ( $\text{sec}^{-1}$ ) for the two alpha groups. Then we equate the constants to the probability flux through a sphere at large  $R$ .

$$\lambda_{18} = u_{18}^* \frac{4\pi}{\mu} \frac{\hbar}{i} \frac{d}{dr} u_{18} \quad (10a)$$

$$\lambda_{15} = u_{15}^* \frac{4\pi}{\mu} \frac{\hbar}{i} \frac{d}{dr} u_{15} \quad (10b)$$

Substituting from Eqs. (3) into Eqs. (10a) and (10b) and using the asymptotic forms for the coulomb functions we obtain

$$\lambda_{18} = 4\pi A^2 \frac{\hbar k_{18}}{\mu} = 4\pi A^2 v_{18} \quad (10c)$$



$$\lambda_{15} = 4\pi B^2 \frac{\hbar k_{15}}{\mu} = 4\pi B^2 v_{15} \quad (10b)$$

where  $v_{13}$  and  $v_{15}$  are the velocities of the respective alpha groups at infinity. From the experimental values of  $\lambda$ 's and  $v$ 's we calculate

$$A = 2.2 \times 10^{-12} \text{Fm}^{-1/2}$$

$$B = 2.3 \times 10^{-13} \text{Fm}^{-1/2}$$

#### 4. Alpha Rate Theory Including Electromagnetic and Nuclear Force Coupling

If we wish to continue the alpha wave functions into the region of the nuclear force field, we must make more specific assumptions about models.

As to the electric  $2^\lambda$ -pole coupling terms, we might assume the source currents to be on a sphere in the nuclear surface region. Then the coupling potential with radial dependence of  $r^{-\lambda-1}$  outside joins continuously at the sphere to an  $r^\lambda$  dependence inside.

The most fundamental form of nuclear potential for the alpha particle would sum over various nucleon-nucleon coördinates in a microscopic fashion. A simpler approximate procedure that may be realistic for collective "shape vibrational" states would be to describe the alpha-nuclear potential in terms of collective shape coördinates. Consider in the case of  $^{208}\text{Pb}$  and an alpha particle a shape-dependent nuclear potential

$$V_\alpha(r, \theta, \phi, \alpha_{3\nu}) = \frac{-V_0}{1 + \exp\left[\frac{r - R(\theta, \phi, \alpha_{3\nu})}{d}\right]} \quad (11a)$$

with

$$R(\theta, \phi, \alpha_{3\nu}) = R_0 [1 + \sum_{\nu} \alpha_{3\nu} Y_{3\nu}^*(\theta, \phi)] \quad (11b)$$

We consider the first-excited 3- state of  $^{208}\text{Pb}$  as the first octupole shape oscillation excitation and have earlier derived <sup>20)</sup> the coupled radial equations for alpha decay for the ground state of  $^{212}\text{Po}$ . These equations we modified for the case of the high spin isomer calculations of this paper. In the course of writing this paper we noted that Tamura has given <sup>21)</sup> very comprehensive and general formulations of the problem. Aside from differences in notation we find our formulas identical to the appropriate special cases of his. Hence, we shall refer for derivations to Tamura's work.

To include the nuclear potential coupling in our eqs. (6a) and (6b) it is only necessary to add to the electromagnetic coupling term (6c) the nuclear coupling term given by Tamura's eq. (27), although we must multiply his coupling matrix element by  $i^{\ell-\ell'} = (-)^{(\ell-\ell')/2}$  since we use ordinary spherical harmonics  $Y_{\ell}^m$  and he uses  $i^{\ell} Y_{\ell}^m$ .

$$(-)^{\frac{\ell-\ell'}{2}} \langle \ell j I | V_{\text{coupl}} | \ell' j' I' \rangle = (-)^{\frac{\ell-\ell'}{2}} \sum_{t, \lambda} v_{\lambda}^{(t)}(r) \langle I || Q_{\lambda}^{(t)} || I' \rangle A(\ell j I, \ell' j' I', \lambda J)$$

In our special case of eqns. (6), the alpha spin  $S$  is zero; the multipolarity  $\lambda = 3$ ;  $\ell = j = 18$ ;  $\ell' = j' = 15$ ; the total angular momentum  $J = 18$ ; the final nuclear spin states are  $I = 0$ ,  $I' = 3$ ; the tensorial rank  $t = 1$  is considered.

Therefore, by Tamura's eq. (29.2), assuming the  $\ell\ell'$  therein is a typographical error for  $2\ell'$  we get

$$A(13\ 18\ 0, 15\ 15\ 3; 3\ 18\ 0)$$

$$= i \left( \frac{31}{4\pi \cdot 7} \right)^{1/2} (18\ 15\ 00|30)$$

The Racah coefficient in Tamura's equation for our case has a zero as one argument, and we replaced it above by the equivalent algebraic factor.

In Bohr's model<sup>22)</sup> of irrotational vibrations of a uniformly charged spherical nucleus, the reduced electric matrix elements are given in terms of surface phonon oscillator constants. From this relationship we can express the reduced matrix element as follows:

$$|\langle I \| Q_3^{(1)} \| I' \rangle|^2 = (2I+1)B(E3; I \rightarrow I') \left( \frac{4\pi}{3ZeR_e^3} \right)^2,$$

where  $R_e$  is the radius of the equivalent uniformly charged sphere ( $\sim 7.5$  Fm). This equation differs from that of Tamura's<sup>21)</sup> footnote 18a only by the squared factor.

His  $v_\lambda^{(1)}(r)$  is given in his eq. (13.1); in our case the nuclear potential is purely real and becomes just the first term of his eq. (13.1). Thus we take  $v_3^{(1)}(r)$  as just  $R_0$  times the first radial derivative of the real Woods-Saxon potential designated  $V_{\text{nuc}}$ ; the coupling term is very nearly a Gaussian peaking on the nuclear surface.

Finally, combining the above expressions we get the nuclear coupling term to add to the electromagnetic coupling term of our eq. (6c).

$$K_{\text{nuc}}(r) = -R_0 \frac{dV_{\text{nuc}}}{dr} \left( \frac{4\pi}{3ZeR_e^2} \right)^2 \gamma [B(E3; 0 \rightarrow 3)]^{1/2} \left( \frac{31}{4\pi \cdot 7} \right)^{1/2} (18 \ 15 \ 00 | 30), \quad (12)$$

where we insert a factor  $\gamma$  to allow for possible deviations from the vibrational model.

It should be understood that the relationship between  $B(E\lambda)$  and the electric coupling matrix element in (6c) is exact in the long-wave-length limit. (If the distances over which the alpha-nuclear coupling is effective are not small compared to the wave length of the photon of energy equal to the nuclear transition energy, then a more complicated expression based on a retarded potential would be necessary. For our case the reduced wave length  $\lambda$  of a 2.615 McV photon is 75 Fm and integrations were carried only from 40 Fm inward.) However, the relationship of eq. (12) is model-dependent, depending on the assumption that the 3- excitation of  $^{208}\text{Pb}$  is an octupole oscillation of a nuclear fluid of constant proton-to-neutron ratio. The factor  $\gamma$  might be less than unity if the microscopic description gave a predominant share of excitation to protons, and, conversely, the factor  $\gamma$  could be greater than unity if the 3- excitation was predominantly neutron-excitation.

We note that the signs of the nuclear and the electromagnetic coupling terms are everywhere opposite to one another. This result accords with the qualitative argument that an excursion of the nuclear surface toward the alpha near the nucleus produces a lowered nuclear potential energy and a more repulsive electrostatic potential energy.

There is a subtle point to be noted regarding the proper sign of the square root of  $B(E3)$  in eqs. (7) and (12). In section 2. of this paper we gave

the microscopic wave functions used for the  $3^-$  state of  $^{208}\text{Pb}$ . The choice of overall sign of these wave functions is completely arbitrary. However, once the choice is made the sign of the electric octupole matrix element is fixed, determining the sign of the coupling term of eq. (12); also the choice fixes the sign of the reduced alpha width to the  $3^-$  state. With our arbitrary choice of phases for the parent  $13^+$  and daughter  $3^-$  wave function as listed in the first section, the  $\gamma_{\alpha L}$  values have the signs shown in Table I and we must take the plus sign for the electric octupole matrix element  $[B(E3)]^{1/2}$  in eqns. (7) and (12). Thus, the final theoretical results of a coupled-equation calculation with the microscopic boundary condition are, as they must be, independent of choice of phase of the shell model wave functions.

### 5. Numerical Solutions of Coupled Equations

We now present the results of inward numerical integrations of the two coupled radial eqs. (6), where the coupling matrix element  $K_{03}$  is the sum of electromagnetic (eq. (7)) and nuclear (eq. (12)) terms. The nuclear potential of eqs. (11) was used with  $V_0 = 35.0$  MeV,  $d = 0.576$  Fm, and  $R_0 = 9.10$  Fm. A model-dependence factor  $\gamma$  of 2.7 was used in order to see the effect of very strong surface coupling. A second calculation was made with  $\gamma = 1$ , and a third with  $V_0 = 74.0$  MeV,  $d = 0.565$  Fm, and  $R_0 = 8.53$  Fm and  $\gamma = 2.7$  as above. The electric coupling term has radial dependence  $r^{-4}$  outside  $R_e = 7.5$  Fm and  $r^3$  inside. (cf. Tamura's eq. (13.1)).

The boundary conditions of Table IV were used, and the resulting amplitudes near the nuclear surface for the four linearly independent basis solutions are given in Tables V, VI, and VII. In the absence of coupling, solutions II and IV based on the regular solutions should be extremely small, and indeed could not be calculated by inward integration, since rounding errors would grow exponentially in the barrier region. However, with coupling present the variations of magnitude of all wave amplitudes is not so great, and the significance of the final results should not be seriously altered by rounding errors. The program was checked by running calculations with coupling turned off and demanding that solutions based on the regular  $F_L$  coulomb function boundary conditions be much less than those based on irregular  $G_L$ .

Using the experimental decay rates of  $^{212m}\text{Po}$  to ground and 3- state and eqs. (10c), (10d), and (9) we solve for the phase shifts due to coupling. There are two acceptable sets:  $\delta_{18} = 33^\circ 10'$  with  $\delta_{15} \approx 0^\circ$  and  $\delta_{18} = 213^\circ 10'$  with  $\delta_{15} \approx 0^\circ$ .

The phase shifts are essentially the same for the calculation with different  $V_0$ , for the phase shifts are mainly determined by coupling strength and potential energies in the vicinity of the outer classical turning point.

With these phases we calculate the real parts of the acceptable solutions by the appropriate linear combination of basis solutions as follows:

$$\begin{aligned} \text{Re}(u_L) = & A[u_L^{(I)} \cos \delta_{18} - u_L^{(II)} \sin \delta_{18}] \\ & + B[u_L^{(III)} \cos \delta_{15} - u_L^{(IV)} \sin \delta_{15}] \end{aligned} \tag{13}$$

Table 5

Basis sets, wave amplitudes, 2 channel case.

		$\gamma = 2.7, V_0 = 35.0 \text{ MeV}$				
B. C.*	L	Radius 6.1 Fm	7.1	8.1	9.1	10.1
I	18	$-5.6182 \times 10^{11}$	$-5.5269 \times 10^{10}$	$-7.0773 \times 10^9$	$-6.8428 \times 10^8$	$-6.7685 \times 10^7$
II	18	$3.6619 \times 10^{11}$	$3.6024 \times 10^{10}$	$4.6134 \times 10^9$	$4.4617 \times 10^8$	$4.4133 \times 10^7$
III	18	$1.2860 \times 10^{13}$	$1.2634 \times 10^{12}$	$1.5828 \times 10^{11}$	$1.1994 \times 10^{10}$	$4.5038 \times 10^8$
IV	18	$-1.7562 \times 10^{10}$	$-1.7254 \times 10^9$	$-2.1616 \times 10^8$	$-1.6374 \times 10^7$	$-6.1319 \times 10^6$
I	15	$2.7410 \times 10^{11}$	$3.9089 \times 10^{10}$	$5.9410 \times 10^9$	$4.6448 \times 10^8$	$1.6724 \times 10^7$
II	15	$-1.7865 \times 10^{11}$	$-2.5477 \times 10^{10}$	$-3.8719 \times 10^9$	$-3.0255 \times 10^8$	$-1.0844 \times 10^7$
III	15	$-6.4028 \times 10^{12}$	$-9.1594 \times 10^{11}$	$-1.4368 \times 10^{11}$	$-1.5061 \times 10^{10}$	$-1.6346 \times 10^9$
IV	15	$8.7445 \times 10^9$	$1.2509 \times 10^9$	$1.9624 \times 10^8$	$2.0577 \times 10^7$	$2.2346 \times 10^6$

\* Boundary conditions, see Table IV.



Table 6

Basis sets, wave amplitudes, 2 channel case.

---

$\gamma = 1.0; V_0 = 35.0 \text{ MeV}$

B. C. L	6.1	7.1	8.1	9.1	10.1
I 18	-2.259 (11)	-2.300 (10)	-3.622 (9)	-5.415 (8)	-6.611 (7)
II 18	1.473 (11)	1.500 (10)	2.362 (9)	3.533 (8)	4.315 (7)
III 18	3.173 (12)	3.195 (11)	4.500 (10)	4.027 (9)	1.553 (8)
IV 18	-4.330 (9)	-4.360 (8)	-6.139 (7)	-5.485 (6)	-2.098 (5)
I 15	6.466 (10)	9.708 (9)	1.700 (9)	1.572 (8)	5.847 (6)
II 15	-4.212 (10)	-6.325 (9)	-1.107 (9)	-1.021 (8)	-3.746 (6)
III 15	-1.905 (12)	-2.953 (11)	-6.321 (10)	-1.143 (10)	-1.594 (9)
IV 15	2.602 (9)	4.034 (8)	8.636 (7)	1.563 (7)	2.179 (6)

---

Table 7  
Basis sets, wave amplitudes, 2 channel case.

---

---

		$\gamma = 2.7 \quad V_0 = 74.0 \text{ MeV}$				
B.	C. L.	6.1	7.1	8.1	9.1	10.1
I	18	-8.2561 (10)	-5.7765 (10)	-1.0881 (10)	-7.2861 (8)	-6.8738 (7)
II	18	5.3812 (10)	3.7650 (10)	7.0916 (9)	4.7507 (8)	4.4857 (7)
III	18	1.9023 (12)	1.3343 (12)	2.5390 (11)	1.2849 (10)	3.6252 (8)
IV	18	-2.5980 (9)	-1.8222 (9)	-3.4677 (8)	-1.7541 (7)	-4.9300 (5)
I	15	2.9143 (10)	4.7744 (10)	1.0307 (10)	5.1116 (8)	1.3568 (7)
II	15	-1.8995 (10)	-3.1118 (10)	-6.7180 (9)	-3.3297 (8)	-8.7831 (6)
III	15	-6.7788 (11)	-1.1043 (12)	-2.3540 (11)	-1.6049 (10)	-1.6605 (9)
IV	15	9.2580 (8)	1.5028 (9)	3.2149 (8)	2.1925 (7)	2.2701 (6)

---

---

Tables 8, 9, and 10 give the values of the real parts of the L=18 and L=15 coupled alpha waves at various radial distances for the two phase choices satisfying experimental intensities and for the three different choices of nuclear potential parameters.

Table 8

Real part of alpha wave amplitudes near the nucleus for  
 $V_0 = 35.0$  MeV and  $\gamma = 2.7$ .

R	$\delta_{18} = 33^\circ 10'$ $\delta_{15} \approx 0^\circ$			$\delta_{18} = 213^\circ 10'$ $\delta_{15} \approx 0^\circ$		
	Re ( $u_{18}$ )	Re ( $u_{15}$ )	Ratio	Re ( $u_{18}$ )	Re ( $u_{15}$ )	Ratio
6.1 Fm	1.49 (0)	-1.18 (0)	-1.26	4.43 (0)	-1.77 (0)	-2.51
7.1 Fm	1.35 (-1)	-1.08 (-1)	-1.25	4.25 (-1)	-3.14 (-1)	-1.35
8.1 Fm	1.79 (-2)	-1.43 (-2)	-1.24	5.50 (-2)	4.87 (-2)	-1.13
9.1 Fm	9.60 (-4)	-2.24 (-3)	-0.429	4.56 (-3)	-4.68 (-3)	-0.97
10.1 Fm	-7.89 (-5)	-3.32 (-4)	-0.238	2.82 (-4)	-4.20 (-4)	-0.67

Table 9

Real part of alpha wave amplitudes near the nucleus for  
 $V_0 = -35.0$  MeV and  $\gamma = 1.0$

R	$\delta_{18} = 33^\circ 10'$ $\delta_{15} \approx 0^\circ$			$\delta_{18} = 213^\circ 10'$ $\delta_{15} \approx 0^\circ$		
	Re ( $u_{18}$ )	Re ( $u_{15}$ )	Ratio	Re ( $u_{18}$ )	Re ( $u_{15}$ )	Ratio
6.1 Fm	1.35 (-1)	-2.67 (-1)	-0.51	1.29 (0)	-6.07 (-1)	-2.12
7.1 Fm	1.30 (-2)	-4.25 (-2)	-0.306	1.34 (-1)	-9.35 (-2)	-1.43
8.1 Fm	8.2 (-4)	-1.00 (-2)	+0.082	1.98 (-2)	-1.90 (-2)	-1.04
9.1 Fm	-2.09 (-4)	-2.22 (-3)	+0.094	2.07 (-3)	-2.94 (-3)	-0.70
10.1 Fm	-1.43 (-4)	-3.51 (-4)	+0.404	2.12 (-4)	-5.19 (-4)	-0.408

Table 10  
 $V_0 = -74.0$  MeV and  $\gamma = 2.7$

R	$\delta_{18} = 33^\circ 10'$ $\delta_{15} \approx 0^\circ$			$\delta_{18} = 213^\circ 10'$ $\delta_{15} \approx 0^\circ$		
	Re ( $u_{18}$ )	Re ( $u_{15}$ )	Ratio	Re ( $u_{18}$ )	Re ( $u_{15}$ )	Ratio
6.1	2.18 (-1)	-3.00 (-2)	-2.72	6.54 (-1)	-2.32 (-1)	-2.82
7.1	1.68 (-1)	-1.28 (-1)	-1.31	4.44 (-1)	-3.80 (-1)	-1.17
8.1	2.99 (-2)	-2.69 (-2)	-1.11	8.71 (-2)	-8.11 (-2)	-1.07
9.1	8.40 (-4)	-2.35 (-3)	-0.36	4.68 (-3)	-5.05 (-3)	-0.93
10.1	-9.65 (-5)	-3.69 (-4)	0.26	1.56 (-4)	-4.19 (-4)	-0.37
11.1	-1.934 (-5)	-4.91 (-5)	0.34	1.06 (-5)	-5.02 (-5)	-0.21
12.1	-2.91 (-6)	-7.26 (-6)	0.46	1.21 (-6)	-7.28 (-6)	-0.17
13.1	-4.88 (-7)	-1.24 (-6)	0.39	1.92 (-7)	-1.24 (-6)	-0.16
14.1	-9.36 (-8)	-2.40 (-7)	0.39	3.64 (-8)	-2.40 (-7)	-0.14
15.1	-2.08 (-8)	-5.27 (-8)	0.39	8.18 (-9)	-5.27 (-8)	-0.16
16.1	-5.21 (-9)	-1.86 (-8)	0.28	2.29 (-9)	-1.86 (-8)	-0.12

The amplitudes are normalized by the absolute decay rates such that when squared and multiplied by  $\Delta r$  in Fm one gets the absolute probability of finding the alpha between spherical surfaces at  $r$  and  $r + \Delta r$ . The square of the amplitude multiplied by  $R_0/4\pi$  is the dimensionless quantity called "surface probability" and tabulated at 9.3 Fm for even-even ground state transitions in Table 7 of Perlman and Rasmussen<sup>23</sup>).

To display the effects of coupling on the wave amplitudes we have plotted in figs. 2 and 3 the ratios  $u_{18}/u_{15}$  at various radial distances. The three coupled solutions are shown along with the ratio for no coupling, and in the lower part of the graph we show the ratios given by the microscopic shell-model calculation (Table 1). One sees that even with coupling, the microscopic theory gives too low  $u_{15}$  amplitude at the larger radii, but it appears that a choice of a small  $R_0$  value reduces the discrepancy markedly. The most favorable situation occurs for the cases of the deepest potential (74 MeV) and the strongest surface coupling ( $\gamma = 2.7$ ). There is, surprisingly, not much difference at radii less than 8 Fm between the amplitude ratios of the  $\delta_{18} = 33^\circ$  and  $\delta_{18} = 213^\circ$  solutions for the deep potential and strong coupling.

One is restrained from inward extrapolation of the  $\gamma_L$  ratios in figs. 3 and 4 to get apparent complete agreement at  $R \sim 6$  Fm, for several reasons: (1) Inside the exponential tail region of the nucleon wave functions the  $\gamma_L$  values will greatly fluctuate and microscopic alpha theory has not been formulated for  $R$  in this region. (2) From Tables 8, 9, 10 it is evident that the solutions imply alpha probabilities in excess of unity for the volume outside 6 Fm, and the solutions at such small radius must therefore have no physical significance.

## 6. Discussion

By no means can we claim a satisfactory explanation of the large (1.0%) alpha decay group from  $^{212m}\text{Po}$  to the first excited state of  $^{208}\text{Pb}$ . It may well be that the lack of octupole core polarization in the initial wave function is a major cause of the remaining discrepancy. It does, however, seem clear that the connection radius  $R_0$  of microscopic alpha decay theory should be chosen significantly smaller than the values hitherto used (8-10 Fm). If a smaller  $R_0$  is chosen, then the strong alpha-channel coupling involving major collective shape oscillational modes must be taken into account, for our numerical calculations here show substantial effects from coupling to the octupole mode. Not only is the ratio of amplitudes to ground and excited states affected, but also the absolute decay rates will be affected. Since we have not resolved the alpha branching ratio problem, we shall not try to use our numerical solutions for quantitative absolute decay rate calculations. Suffice it to note qualitatively that there are substantial effects of channel coupling on theoretical absolute rates. Note in Tables 8, 9, and 10 that the total alpha probabilities ( $|u_{18}|^2 + |u_{15}|^2$ ) at small radii are usually about an order of magnitude larger for the  $213^\circ$  cases than for the  $33^\circ$  cases. This result means that the effective barrier penetrability in the  $213^\circ$  cases is an order of magnitude smaller than for  $33^\circ$  cases. The effect of the surface coupling potential is to raise the effective barrier for both partial waves in the  $213^\circ$  cases and to lower the barrier for  $33^\circ$  cases.

As mentioned earlier in Sec. 2, Glendenning and Harada calculated theoretical alpha decay ratios between the  $^{212m}\text{Po}$  isomer and the ground state, finding the theoretical relative rate for the isomer too fast by a factor of  $\sim 45$  for

$R_0 = 9.5$  Fm or  $\approx 1S$  for  $R_0 \approx 9.0$  Fm. We noted in Sec. 2 that their apparent discrepancy factor may reverse for  $R_0 < 8$  Fm. A careful recalculation of the decay rate ratio of isomer and ground state might provide the basis to decide between the  $213^\circ$  case and the  $33^\circ$  case. The ground state decay rate is also affected by channel coupling but less than the isomer.

The alpha decay theory applied to high-spin isomers, such as,  $^{212m}\text{Po}$  and  $^{211m}\text{Po}$  is deserving of further study for the light it may shed on fundamentals of the theory. We have argued above for joining bound and open-channel solutions at smaller radii than previous practice; however, such will aggravate the problem of the usual mismatch at  $R_0$  of logarithmic derivatives of the alpha amplitude in inner and outer regions. There is clearly a need to reformulate alpha theory along the lines of Feshbach's "Unified theory of nuclear reactions"<sup>24</sup>), where the arbitrary division of space into inner and outer regions need not be made.

#### 7. Acknowledgments

One of the authors, K. Harada, wishes to express sincere thanks to Professor M. Baranger for the opportunity of studying in his group at the Carnegie Institute of Technology during part of this research project. We are especially grateful to Prof. W. True for making available his unpublished wave functions for  $^{208}\text{Pb}$ .



REFERENCES

- 1) cf. H. J. Mang, Annl. Rev. Nucl. Sci. 14 (1964) 1
- 2) M. A. Preston, Phys. Rev. 75 (1949) 90
- 3) cf. J. O. Rasmussen, Alpha-, Beta- and Gamma - Ray Spectroscopy, North-Holland Publishing Co., Amsterdam, 1965, Ch. 11, p. 701
- 4) J. O. Rasmussen and B. Segall, Phys. Rev. 103 (1956) 1298
- 5) H. J. Mang, Zeits. f. Physik 148 (1957) 572
- 6) J. K. Poggenburg, Ph.D. Thesis, Lawrence Radiation Laboratory Report UCRL-16187 (August 1965) unpublished
- 7) P. O. Fröman, Mat. Fys. Skr. Dan. Vid. Selsk. 1 (1957) no. 3
- 8) N. K. Glendenning and K. Harada, Nucl. Phys. 72 (1965) 481
- 9) I. Perlman, F. Asaro, A. Ghiorso, A. Larsh, and R. Latimer, Phys. Rev. 127 (1962) 917
- 10) L. Mc Fadden and G. R. Satchler, Nucl. Phys. 84 (1966) 177
- 11) H. V. Gillet, A. M. Green, and E. A. Sanderson, Phys. Letters 11 (1964) 44
- 12) W. T. Pinkston, Nucl. Phys. 37 (1962) 312
- 13) W. W. True and W. T. Pinkston, to be published in Phys. Rev.
- 14) H. D. Zeh, Zeits. f. Physik 175 (1963) 490
- 15) J. O. Rasmussen, Nucl. Phys. 44 (1963) 93
- 16) J. Blomqvist and S. Wahlborn, Ark. f. Physik. 16 (1960) no. 46
- 17) R. G. Thomas, Prog. Theor. Phys. (Japan) 12 (1954) 253
- 18) A. M. Lane and E. D. Pendlebury, Nucl. Phys. 15 (1960) 39
- 19) J. O. Rasmussen and E. R. Hansen, Phys. Rev. 109 (1953) 1656

- 20) E. Rauscher, M. S. Thesis, Lawrence Radiation Laboratory Report  
UCRL-11875 (January 1965) unpublished
- 21) T. Tamura, Rev. Mod. Phys. 37 (1965) 679
- 22) A. Bohr and B. R. Mottelson, Mat. Fys. Skr. Dan. Vid. Selsk. 27 (1955)  
no. 16
- 23) I. Perlman and J. O. Rasmussen, "Alpha Radioactivity", Handbuch der Physik,  
(Springer-Verlag, Berlin, 1957), vol. 42
- 24) H. Feshbach, Ann. Phys. 19 (1962) 287

Figure Captions

Fig. 1. Energy levels of  $^{208}\text{Pb}$  and the alpha decay scheme of  $^{212\text{m}}\text{Po}$ .  
(cf. ref. 9)

Fig. 2. Potential energy (including centrifugal term) for various alpha partial waves on  $^{208}\text{Pb}$ .

$$V(R) = \frac{2Ze^2}{R} + \frac{\hbar^2(L+1/2)^2}{2\mu R^2} - V_0 \exp \frac{R-r_0 A^{1/3}-a}{d}^{-1}$$

with

$$V_0 = 35 \text{ MeV}, r_0 = 1.17 \text{ Fm}, a = 2.17 \text{ Fm}, \text{ and } d = 0.576 \text{ Fm}.$$

Fig. 3. Wave amplitude ratio  $\frac{u_{18}}{u_{15}}$  for  $33^\circ 10'$  solutions as a function of radial distance

uncoupled  $V_0 = 35 \text{ MeV}$

coupled  $\gamma = 2.7, V_0 = 35 \text{ MeV}$

coupled  $\gamma = 1.0, V_0 = 35 \text{ MeV}$

coupled  $\gamma = 2.7, V_0 = 74 \text{ MeV}$

$\frac{\gamma_{18}}{\gamma_{15}}$  ratio using shell model wave functions of  
refs. 8 and 12

Fig. 4. Wave amplitude ratio  $\frac{u_{18}}{u_{15}}$  for  $213^\circ 10'$  solutions as a function of radial distance

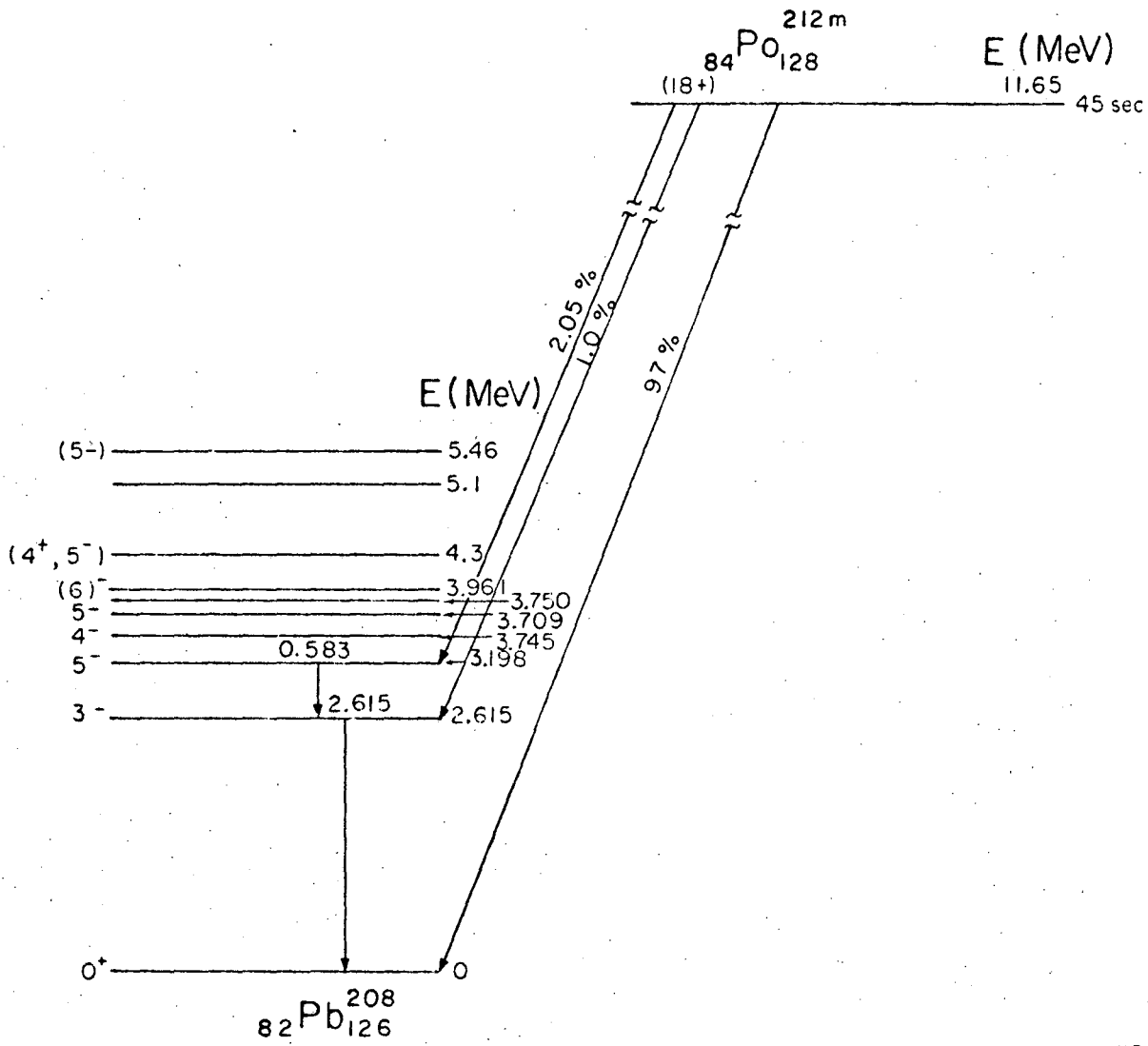
uncoupled  $V_0 = 35 \text{ MeV}$

coupled  $\gamma = 2.7, V_0 = 35 \text{ MeV}$

coupled  $\gamma = 1.0, V_0 = 35 \text{ MeV}$

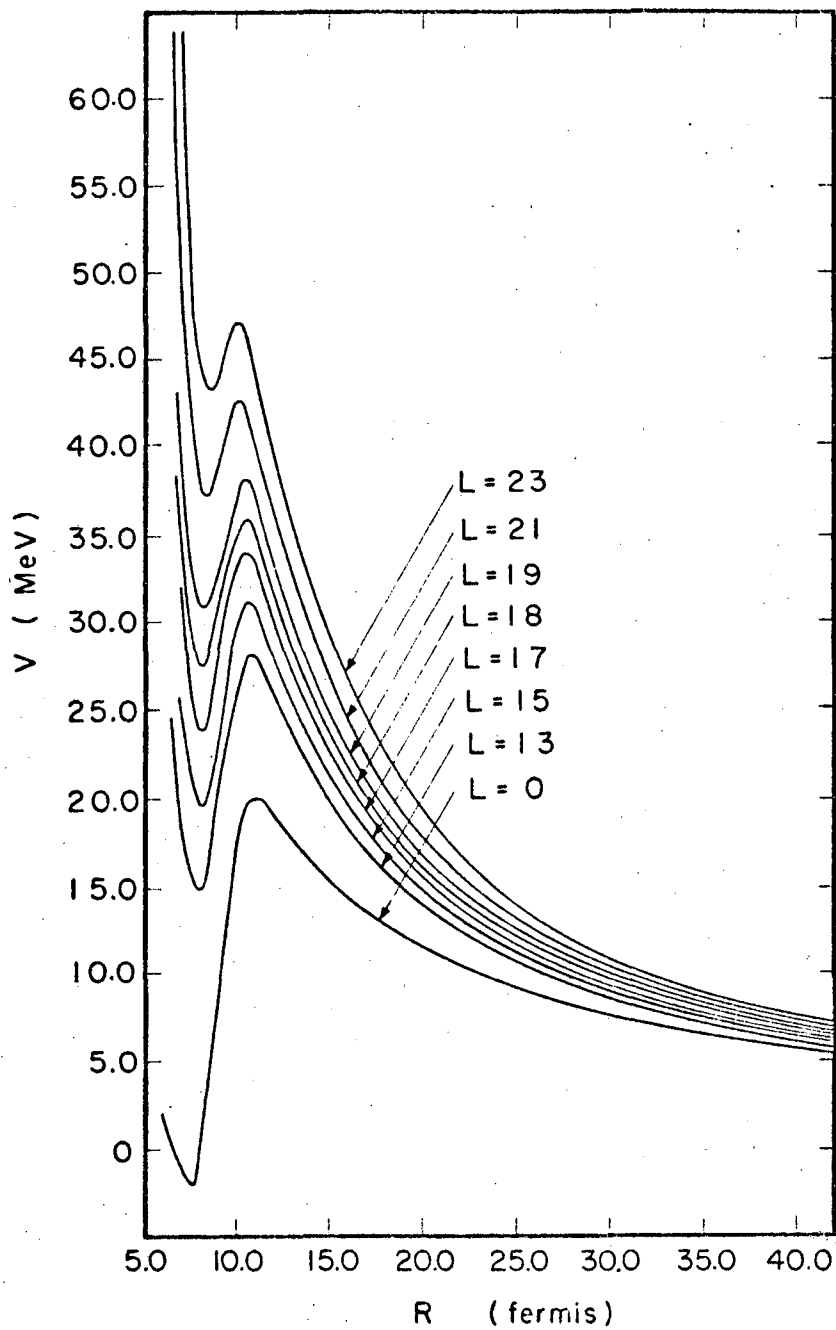
coupled  $\gamma = 2.7, V_0 = 74 \text{ MeV}$

$\frac{\gamma_{18}}{\gamma_{15}}$  ratio using shell model wave functions of  
refs. 3 and 12



MUB-9091

Fig. 1



MUB-9092

Fig. 2

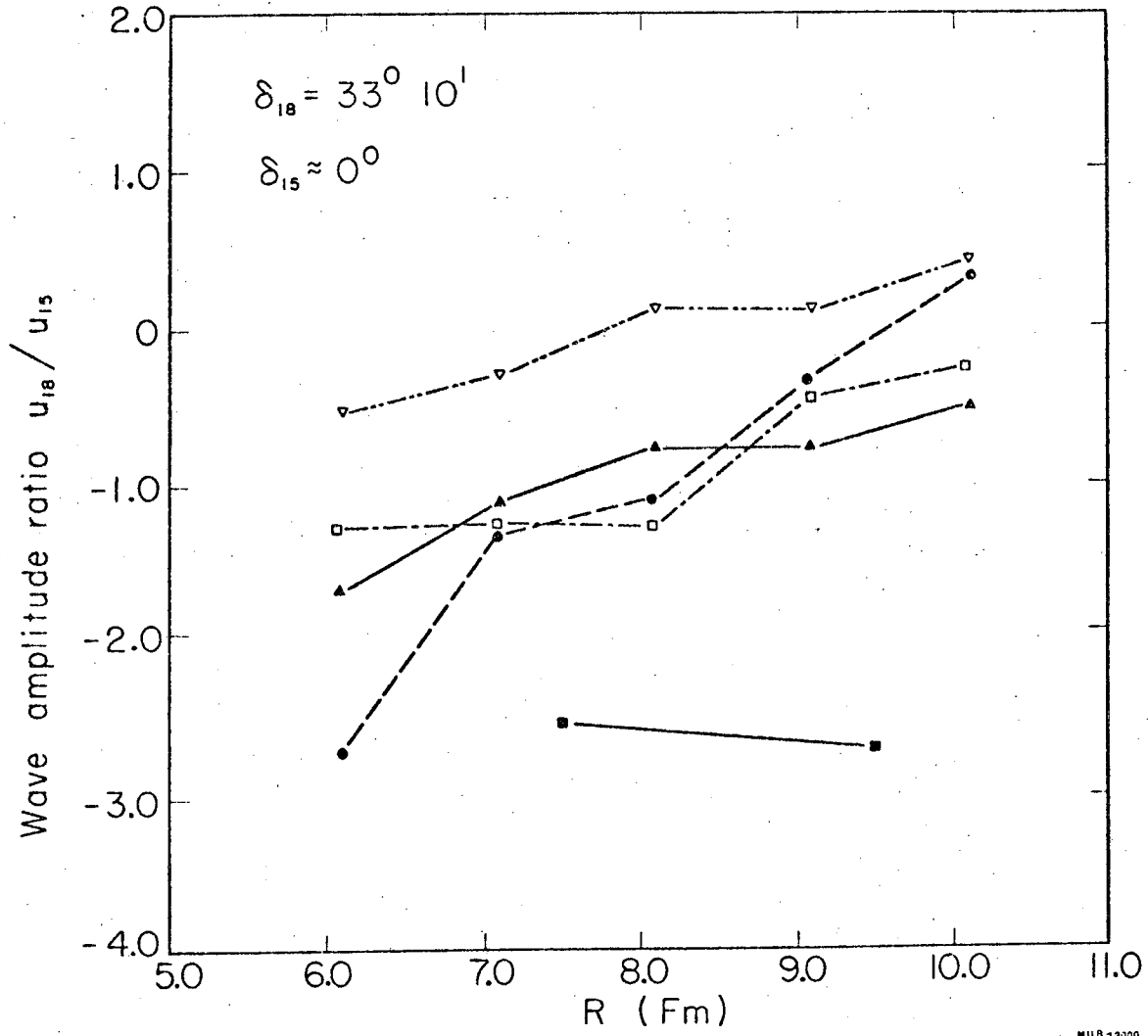


Fig. 3

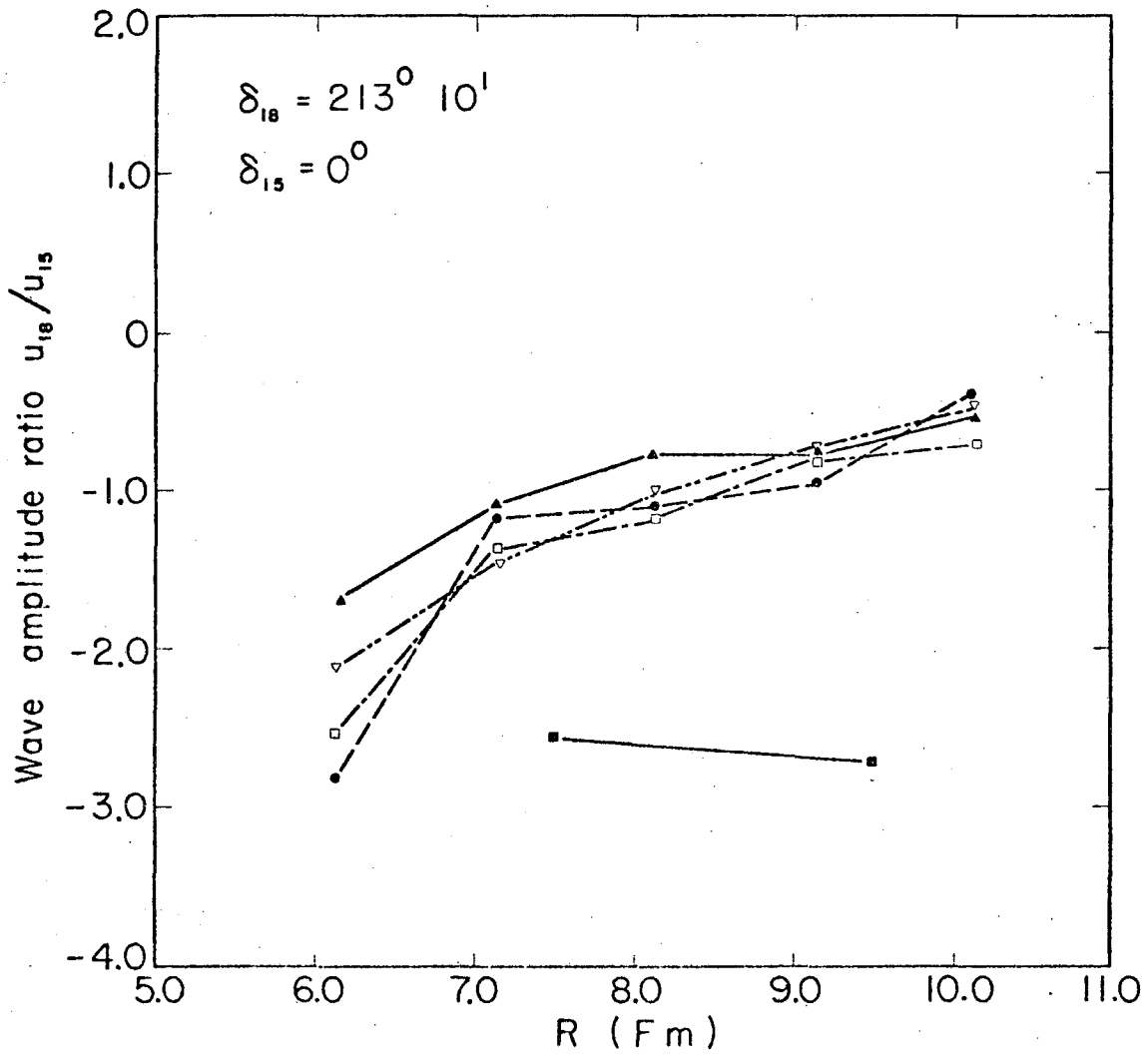


Fig. 4

This report was prepared as an account of Government sponsored work. Neither the United States, nor the Commission, nor any person acting on behalf of the Commission:

- A. Makes any warranty or representation, expressed or implied, with respect to the accuracy, completeness, or usefulness of the information contained in this report, or that the use of any information, apparatus, method, or process disclosed in this report may not infringe privately owned rights; or
- B. Assumes any liabilities with respect to the use of, or for damages resulting from the use of any information, apparatus, method, or process disclosed in this report.

As used in the above, "person acting on behalf of the Commission" includes any employee or contractor of the Commission, or employee of such contractor, to the extent that such employee or contractor of the Commission, or employee of such contractor prepares, disseminates, or provides access to, any information pursuant to his employment or contract with the Commission, or his employment with such contractor.



[Faint, illegible text covering the majority of the page]

